ASME Open Journal of Engineering
Online journal at:
https://asmedigitalcollection.asme.org/openengineering

Transient Response Analysis of Nonlinear Oscillators With Fractional Derivative Elements Under Gaussian White Noise Using Complex Fractional Moments

Takahiro Tsuchida[1]
Department of Systems and Control Engineering,
Tokyo Institute of Technology,
Ookayama 2-12-1, Meguro-ku,
Tokyo 152-8552, Japan
e-mail: ttsuchida@sc.e.titech.ac.jp

Daizoh Itoh
Department of Systems and Control Engineering,
Tokyo Institute of Technology,
Ookayama 2-12-1, Meguro-ku,
Tokyo 152-8552, Japan

Tsubasa Eguchi
Department of Systems and Control Engineering,
Tokyo Institute of Technology,
Ookayama 2-12-1, Meguro-ku,
Tokyo 152-8552, Japan

Complex fractional moment (CFM), which is defined as the Mellin transform of a probability density function (PDF), has been successfully employed to find the response PDF of a wide variety of integer-order nonlinear oscillators. In this paper, a CFM-based analysis is performed to determine the transient response PDF of nonlinear oscillators with fractional derivative elements under Gaussian white noise. First, an equivalent linear system is introduced for the purpose of deriving the Fokker–Planck (FP) equation for response amplitude. The equivalent natural frequency and equivalent damping coefficient of the system need to be determined, taking into account both the nonlinear and fractional derivative elements of the original oscillator. Moreover, to convert the FP equation into the governing equation of CFMs, these equivalent coefficients must be given in polynomial form of amplitude. This paper proposes formulas for appropriately determining the equivalent coefficients, based on an equivalent linearization technique. Then, applying stochastic averaging, the FP equation is derived from the equivalent linear system. Next, the Mellin transform converts the FP equation into coupled linear ordinary differential equations for amplitude CFMs, which are solved with a constraint corresponding to the normalization condition for a PDF. Finally, the inverse Mellin transform of the CFMs yields the amplitude PDF. The joint PDF of displacement and velocity is also obtained from the amplitude PDF. Three linear and nonlinear fractional oscillators are considered in numerical examples. For all cases, the analytical results are in good agreement with the pertinent Monte Carlo simulation results. [DOI: 10.1115/1.4065126]

Keywords: nonlinear random vibration, fractional derivative, complex fractional moment, equivalent linearization, stochastic averaging, transient response probability density

1 Introduction

Mechanical and structural systems in various engineering applications are exposed to random excitations, such as seismic ground motion, fluctuating pressure in turbulent flow, and hydraulic force of ocean waves. In order to grasp the response characteristics of dynamic systems subjected to random excitation and to assess their reliability, it is important to accurately determine the probability density function (PDF) of the system response. For a nonlinear system under Gaussian white noise, the system response can usually be regarded as a Markov process, and the time evolution of the response PDF is governed by a partial differential equation called Fokker–Planck (FP) equation. Unfortunately, exact solutions of the FP equation are not available except for the stationary response of a very limited class of nonlinear systems [1]. Solutions for transient/non-stationary responses are even more difficult to obtain, owing to their time dependence. Therefore, the development of approximate analytical or numerical techniques for finding system response PDFs is a significant issue in the field of stochastic dynamics.

In the last few decades, fractional calculus has attracted a great deal of attention due to its usefulness as a mathematical modeling tool for non-local or long-memory phenomena. Various topics on fractional calculus in science and engineering can be found in the books [2–7] and the papers [8–10]. One successful application of fractional calculus to engineering is the modeling of viscoelastic materials. Indeed, many experimental results have proven that fractional derivative models with a small number of parameters can describe viscoelastic behavior with a high degree of

[1]Corresponding author.

Manuscript received October 10, 2023; final manuscript received March 16, 2024; published online April 9, 2024. Assoc. Editor: Oleg Schilling.

accuracy [11–18]. Therefore, in mechanical and structural dynamics, the fractional models have become widely used as models of viscoelastic dampers for seismic isolation and vibration control [16,19–23].

Under such circumstances, there has been a growing interest in the response determination of dynamic systems with fractional derivative elements under stochastic excitation. In this regard, Monte Carlo simulation (MCS) comes to mind as a general-purpose method. However, computing the fractional derivative operator requires considerable computational time and resources, since this operator is defined by a convolution integral, i.e., depends on the function's entire past time history. Hence, direct numerical integration of system equations with fractional-order derivatives is much more computationally demanding than that of systems with only integer-order derivatives. For this reason, in recent years, a lot of efforts have been put into developing analytical techniques for determining the stochastic response of fractional-order systems. Meanwhile, machines and structures including viscoelastic materials have often been modeled as single-degree-of-freedom (SDOF) systems with fractional derivative elements [2,4,8,9,12–14,16]. Therefore, the development of analytical methods for SDOF systems with fractional derivatives is interesting and important from a practical point of view.

For moment analysis, an approach based on convolutional representation of the response was presented to obtain the response variance of SDOF linear systems with fractional derivatives [24,25]. More recently, approximate closed-form solutions of response moments were obtained for fractional linear oscillators to evolutionary stochastic excitation by expressing their impulse response with Prony series [26]. A moment equation approach has also been employed [27–29], where fractional-order systems are approximately converted into coupled integer-order differential equations. In addition, frequency-domain approaches have been developed for stationary moment analysis [30–32].

For the analysis of PDFs, stochastic averaging has been widely utilized. The displacement and velocity responses of fractional systems are no longer a Markov vector due to the history dependence of the fractional terms, even if the excitation is a white noise process. Nevertheless, by applying stochastic averaging, the response amplitude can be approximately treated as a Markov process, resulting in the FP equation governing the amplitude PDF [33]. As an additional benefit, system dimension reduction is also achieved. In this manner, the amplitude PDF of the stationary response of various fractional nonlinear oscillators has been accurately obtained [33–41].

Compared to moment and stationary PDF analyses, the analysis of transient response PDF is a more difficult task. Although the number of studies is still limited at present, efforts are being made to seek an approximate solution of the transient amplitude PDF of fractional nonlinear systems using a path integral technique [42] or a Rayleigh distribution assumption [43]. However, these existing methods have some drawbacks in terms of computational cost and applicability. The path integration generally requires very short time-steps to obtain a highly accurate solution. The Rayleigh distribution assumption for amplitude PDF may not be appropriate for some types of nonlinear systems, such as oscillators possessing limit cycles. Therefore, it remains an important challenge to develop efficient and versatile analytical methods for determining the transient response PDF of nonlinear oscillators with fractional derivative elements.

Meanwhile, a novel statistical moment named complex fractional moment (CFM) was proposed for the characterization of random variables [44,45]. The CFM is a complex-order moment, which is calculated as the Mellin transform of a PDF. Similar to the Fourier transform relation between PDFs and characteristic functions, the inverse Mellin transform of the CFM reconstructs the original PDF. This striking feature of the CFM allows us to estimate PDFs via CFMs. Di Paola presented a CFM-based approach for solving the FP equation corresponding to first-order nonlinear systems excited by Gaussian white noise [46], in which by applying the Mellin transform to the FP equation, it is converted into a set of linear ordinary differential equations with respect to response CFMs. In other words, a partial differential equation is converted into linear ordinary differential equations much easier to solve. Then, solving the CFM equations and taking the inverse Mellin transform on the resulting CFMs, the response PDF is constructed. Through the above method, the PDFs of both transient and stationary responses were accurately determined in the whole domain, including the tail region. This method has also been applied successfully for white noise excitations of other types [47–49]. Jin et al. developed the CFM-based approach for SDOF oscillators with nonlinear damping under Gaussian white noise by combining stochastic averaging [50]. Stochastic averaging leads to the FP equation for response amplitude, which is then solved via CFMs. The CFM method combined with stochastic averaging yielded transient and stationary response PDFs with high accuracy, and the computational time was significantly reduced compared to the corresponding MCS. In the subsequent studies, this method has been extended to a wide class of integer-order nonlinear oscillators, including systems with nonlinearities in both stiffness and damping [51], nonlinear vibro-impact systems [52] and nonlinear systems with time delay [53]. Such great success of the CFM-based method suggests that it can also be a powerful tool in the transient response analysis of fractional-order nonlinear oscillators.

In this paper, a CFM-based analysis is performed to determine the transient response PDF of nonlinear oscillators with fractional derivative elements, whose nonlinearities are included in both stiffness and damping. This analysis is mainly based on an analytical method for integer-order nonlinear oscillators recently developed by some of the authors [51]. First, we aim to derive the FP equation for response amplitude using stochastic averaging. For this purpose, the equivalent natural frequency and equivalent damping coefficient of the oscillator need to be determined. As an important point in the analysis of fractional oscillators, these equivalent coefficients have to include not only the effects of nonlinearities, but also the contributions of the fractional derivative terms. Furthermore, the coefficients must be given in polynomial form of response amplitude to utilize the CFM-based approach. This paper proposes formulas for determining the equivalent coefficients that satisfy the above requirements, based on an equivalent linearization technique. Then, resorting to stochastic averaging, the FP equation is derived. The solution of the FP equation, i.e., the amplitude PDF, is sought through the CFM approach. The joint PDF of displacement and velocity is also obtained from the amplitude PDF. The accuracy and versatility of the present analytical technique are demonstrated through numerical examples of three linear and nonlinear oscillators with fractional derivatives.

2 Preliminaries

2.1 Mellin Transform. The Mellin transform $M_f(\gamma-1)$ of a real function $f(x)$ with domain $0 \le x < \infty$ is defined as [45]

$$M_f(\gamma-1)=\int_0^\infty x^{\gamma-1}f(x)dx,\quad \gamma=\rho+i\eta \tag{1}$$

where $i=\sqrt{-1}$ and $\rho, \eta \in \mathbb{R}$. The inverse Mellin transform is given in the form

$$f(x)=\frac{1}{2\pi}\int_{-\infty}^{\infty} M_f(\gamma-1)x^{-\gamma}\mathrm{d}\eta,\quad x>0 \tag{2}$$

The integration in Eq. (2) is calculated with respect to the imaginary part η of γ while the real part ρ is fixed. The condition for the existence of the Mellin transform is

$$\begin{cases} -p<\rho<-q \\ \lim\limits_{x\to 0} f(x)=\mathcal{O}(x^p), \qquad \lim\limits_{x\to\infty} f(x)=\mathcal{O}(x^q) \end{cases} \tag{3}$$

where $\mathcal{O}(\cdot)$ denotes the Landau symbol. The range of ρ in Eq. (3) is referred to as *Fundamental Strip* (FS) of the Mellin transform [45].

2.2 Complex Fractional Moment. Let Y be a non-negative random variable with a PDF $p_Y(y)$. The CFM of Y is defined as [45]

$$\mathrm{E}[Y^{\gamma-1}] = \int_0^\infty y^{\gamma-1} p_Y(y) dy = M_{p_Y}(\gamma - 1) \tag{4}$$

where γ is a complex number $\gamma = \rho + i\eta$, $\mathrm{E}[\cdot]$ represents mathematical expectation. As can be seen from Eq. (4), the CFM is given as the Mellin transform of the PDF $p_Y(y)$. Therefore, CFM is henceforth denoted as $M_{p_Y}(\gamma - 1)$. Using the inverse Mellin transform, the PDF $p_Y(y)$ can be reconstructed.

$$p_Y(y) = \frac{1}{2\pi} \int_{-\infty}^{\infty} M_{p_Y}(\gamma - 1) y^{-\gamma} d\eta, \quad y > 0 \tag{5}$$

$p_Y(y)$ is determined from Eq. (5) uniquely, irrespective of the choice of the real part ρ of γ, provided that ρ belongs to the FS [45]. Equation (5) is discretized in preparation for the analysis in Sec. 5.

$$p_Y(y) = \frac{1}{2b} \sum_{s=-m}^{m} M_{p_Y}(\gamma_s - 1) y^{-\gamma_s}, \quad y > 0 \tag{6}$$

where $b = \pi/\Delta\eta$ and $\gamma_s = \rho + is\Delta\eta$. $\Delta\eta$ is the discretization step of η. The value of m defines a cutoff value $\bar{\eta} = m\Delta\eta$. CFM generally converges to zero as $|\eta| \to \infty$ [44], which means that the effect of truncating η in Eq. (6) is negligible if a sufficiently large $\bar{\eta}$ is chosen.

3 Equation of Motion

Consider an SDOF nonlinear oscillator with a fractional derivative element. The system equation of motion is given by

$$\ddot{X} + \varepsilon\lambda D^{\alpha}_{0,t} X + \varepsilon h(X, \dot{X}) + \omega_0^2 X + \varepsilon\omega_0^2 g(X) = \varepsilon^{\frac{1}{2}} W(t) \tag{7}$$

where X denotes the system displacement. The dot symbol represents the (integer-order) derivative with respect to time t. $h(X, \dot{X})$ and $g(X)$ are nonlinear functions that account for the nonlinearities of damping and stiffness, respectively. $W(t)$ is a zero-mean Gaussian white noise of power spectral density S_0 and is suddenly applied to the system at $t = 0$. λ is a coefficient, and $D^{\alpha}_{0,t} X$ denotes the Caputo fractional derivative of order $0 < \alpha < 1$ of $X(t)$ defined as [2]

$$D^{\alpha}_{0,t} X(t) = \frac{1}{\Gamma(1-\alpha)} \int_0^t \frac{\dot{X}(s)}{(t-s)^{\alpha}} ds \tag{8}$$

where $\Gamma(\cdot)$ is the gamma function. The fractional derivative term with $0 < \alpha < 1$, which is commonly referred to as "springpot," represents viscoelastic damping force that is intermediate between the elastic force of a spring ($\alpha = 0$) and the viscous damping force of a dashpot ($\alpha = 1$). This term behaves more like a spring as α approaches 0, whereas dashpot-like behavior prevails when α is close to 1. The parameter $\varepsilon > 0$ is employed to quantify the magnitude of the fractional derivative, nonlinear damping, nonlinear stiffness, and excitation terms. ω_0 is the natural frequency of the corresponding linear system ($\varepsilon = 0$). The system (7) is quiescent for $t \le 0$.

Assume that $h(X, \dot{X})$ is a polynomial of the form

$$h(X, \dot{X}) = \sum_{i=1} c_i X^{n_i} \dot{X}^{2m_i+1}, \quad n_i, \ m_i \in \mathbb{Z}_{\ge 0} \tag{9}$$

where c_i are coefficients, and $\mathbb{Z}_{\ge 0}$ denotes the set of non-negative integers. From Eq. (9), the order of $\dot{X}$ in $h(X, \dot{X})$ is odd. Equation (9) includes various nonlinear damping models for dynamic systems of engineering interest, e.g., damping of ship roll motion [54] and energy-dependent damping [55]. Furthermore, Eq. (9) also includes nonlinear damping for oscillators exhibiting limit-cycle behavior such as the van der Pol oscillator. Thus, Eq. (9) can represent the damping nonlinearities of diverse oscillatory systems. It is also assumed that $g(X)$ is given by a polynomial of X.

The purpose of this paper is to obtain the transient response PDF of the oscillator expressed by Eq. (7). Some of the authors recently developed a CFM-based analytical approach for determining the transient response PDF of an integer-order nonlinear oscillator obtained by removing the fractional derivative term from Eq. (7) [51]. The present analysis for the fractional nonlinear oscillator (7) is also performed based on this analytical approach. An important point that must be addressed to accomplish this analysis is the appropriate determination of the equivalent natural frequency and equivalent damping coefficient for the fractional nonlinear oscillator.

4 Derivation of Fokker–Planck Equation for Response Amplitude

4.1 Pseudo-Harmonic Representation of Response. Assuming that $\varepsilon \ll 1$, the response of the oscillator of Eq. (7) exhibits pseudo-harmonic behavior. Thus, $X(t)$ and $\dot{X}(t)$ are described by the following equations [33,42,43]:

$$\begin{aligned} X(t) &= A(t)\cos\left(\omega_e(A)t + \Phi(t)\right) \\ \dot{X}(t) &= -A(t)\omega_e(A)\sin\left(\omega_e(A)t + \Phi(t)\right) \end{aligned} \tag{10}$$

where $A(t)$ and $\Phi(t)$ are amplitude and phase, respectively, which are slowly varying functions of time t. $\omega_e(A)$ is an equivalent natural frequency of the oscillator, which depends on $A(t)$. In Ref. [51], $\omega_e(A)$ was determined considering the effect of nonlinear stiffness. For the fractional oscillator under study, its fractional derivative (viscoelastic) element contributes to both elasticity and viscosity. Therefore, $\omega_e(A)$ needs to be determined by taking account of both the stiffness nonlinearity and the elastic contribution of the fractional element. To this aim, we propose a formula for determining $\omega_e(A)$ based on an equivalent linearization technique.

4.2 Equivalent Linearization. An equivalent linear system for the original oscillator (7) is introduced, whose equation of motion is given as

$$\ddot{X} + \varepsilon\beta_e(A)\dot{X} + \omega_e^2(A)X = \varepsilon^{\frac{1}{2}} W(t) \tag{11}$$

where $\omega_e(A)$ is an equivalent natural frequency. $\beta_e(A)$ is an equivalent damping coefficient, depending on the amplitude $A(t)$. Similarly to $\omega_e(A)$, we determine $\beta_e(A)$ by taking into account both the nonlinear damping and the contribution of the fractional (viscoelastic) term to viscous damping. The equivalent system behaves in a pseudo-harmonic manner. In other words, the response of the system (11) is given by Eq. (10).

In the equivalent linearization technique, the equivalent coefficients $\omega_e(A)$ and $\beta_e(A)$ are selected according to some statistical criterion. In this paper, the criterion of least mean square error is used. Thus, $\omega_e(A)$ and $\beta_e(A)$ are determined in such a way that the mean square error between the original oscillator (7) and the equivalent linear system (11) is minimized. Performing a mean square minimization procedure [56–58] on the error between Eqs. (7) and (11) yields $\omega_e(A)$ and $\beta_e(A)$ in the form

$$\begin{aligned} \omega_e^2(A) = \omega_0^2 \left\{ 1 + \frac{\varepsilon}{\pi A} \int_0^{2\pi} g(A\cos\psi)\cos\psi d\psi \right\} \\ + \frac{\varepsilon\lambda}{\pi} \int_0^{2\pi} (D^{\alpha}_{0,t} \cos\psi)\cos\psi d\psi \end{aligned} \tag{12}$$

and

$$\begin{aligned} \beta_e(A) = -\frac{1}{\pi\omega_e(A)A} \int_0^{2\pi} h(A\cos\psi, \ -A\omega_e(A)\sin\psi)\sin\psi d\psi \\ - \frac{\lambda}{\pi\omega_e(A)} \int_0^{2\pi} (D^{\alpha}_{0,t} \cos\psi)\sin\psi d\psi \end{aligned} \tag{13}$$

where $\psi = \omega_e(A)t + \Phi$. In deriving Eqs. (12) and (13), $A(t)$ and $\Phi(t)$ were considered constant during one period of oscillation, and the fact that $h(X, \dot{X})$ is given by Eq. (9) was employed. The integrals involving fractional derivatives in Eqs. (12) and (13) can be calculated as follows [43]:

$$\int_0^{2\pi} (D_{0,t}^{\alpha} \cos\psi)\cos\psi d\psi = \pi\omega_e^{\alpha}(A)\cos\left(\frac{\alpha\pi}{2}\right) \tag{14}$$

$$\int_0^{2\pi} (D_{0,t}^{\alpha} \cos\psi)\sin\psi d\psi = -\pi\omega_e^{\alpha}(A)\sin\left(\frac{\alpha\pi}{2}\right) \tag{15}$$

Then, Eqs. (12) and (13) become

$$\omega_e^2(A) = \omega_0^2\left\{1 + \varepsilon\frac{1}{\pi A}\int_0^{2\pi} g(A\cos\psi)\cos\psi d\psi\right\} + \varepsilon\lambda\omega_e^{\alpha}(A)\cos\left(\frac{\alpha\pi}{2}\right) \tag{16}$$

and

$$\beta_e(A) = -\frac{1}{\pi\omega_e(A)A}\int_0^{2\pi} h(A\cos\psi,\ -A\omega_e(A)\sin\psi)\sin\psi d\psi + \lambda\omega_e^{\alpha-1}(A)\sin\left(\frac{\alpha\pi}{2}\right) \tag{17}$$

To solve the FP equation derived in the following section via the CFM-based approach, $\omega_e^2(A)$ and $\beta_e(A)$ must be given as polynomials in amplitude A [51]. Unfortunately, this requirement is not met, due to the presence of $\omega_e^{\alpha}(A)$ and $\omega_e^{\alpha-1}(A)$ in Eqs. (16) and (17) $(0 < \alpha < 1)$. In order to overcome this problem, $\omega_e^{\alpha}(A)$ in Eq. (16) and $\omega_e^{\alpha-1}(A)$ in Eq. (17) are approximated by ω_0^{α} and $\omega_0^{\alpha-1}$, respectively. This analysis assumes $\varepsilon \ll 1$. In Eq. (16), the term to which the approximation is made includes ε. On the other hand, Eq. (17) does not include ε, but the damping term of the equivalent linear system in Eq. (11) is multiplied by ε. Therefore, the effect of the approximation is considered sufficiently small.

Finally, the formulas for determining $\omega_e(A)$ and $\beta_e(A)$ in the present analysis are as follows:

$$\omega_e^2(A) = \omega_0^2\left\{1 + \varepsilon\frac{1}{\pi A}\int_0^{2\pi} g(A\cos\psi)\cos\psi d\psi\right\} + \varepsilon\lambda\omega_0^{\alpha}\cos\left(\frac{\alpha\pi}{2}\right) \tag{18}$$

and

$$\beta_e(A) = -\frac{1}{\pi\omega_e(A)A}\int_0^{2\pi} h(A\cos\psi,\ -A\omega_e(A)\sin\psi)\sin\psi d\psi + \lambda\omega_0^{\alpha-1}\sin\left(\frac{\alpha\pi}{2}\right) \tag{19}$$

The last constant terms in Eqs. (18) and (19) represent the elastic and viscous contributions of the fractional element, respectively. Substituting these equivalent coefficients into Eq. (11) yields an equivalent linear system for the original fractional nonlinear oscillator. Subsequent analysis proceeds in the same manner as in Ref. [51].

4.3 Stochastic Averaging. Using Eqs. (10) and (11), the first-order differential equation for the response amplitude $A(t)$ is derived as [51]

$$\dot{A} = -\varepsilon\beta_e(A)A\sin^2(\omega_e(A)t + \Phi) - \varepsilon^{\frac{1}{2}}\frac{\sin(\omega_e(A)t + \Phi)}{\omega_e(A)}W(t) \tag{20}$$

Herein, Eq. (20) is decoupled from the phase $\Phi(t)$ by utilizing stochastic averaging [59,60]. Then, $A(t)$ is described by the following one-dimensional stochastic differential equation:

$$\dot{A} = -\frac{\varepsilon\beta_e(A)A}{2} + \frac{\varepsilon\pi S_0}{2A\omega_e^2(A)} + \sqrt{\frac{\varepsilon\pi S_0}{\omega_e^2(A)}}\xi(t) \tag{21}$$

where $\xi(t)$ is a zero-mean delta-correlated process of unit intensity (i.e., $\mathrm{E}[\xi(t)\xi(t+\tau)] = \delta(\tau)$, in which $\delta(\cdot)$ is the Dirac delta function).

Equation (21) is a stochastic differential equation in the Stratonovich sense. Considering the so-called Wong–Zakai correction term, the FP equation corresponding to Eq. (21) is derived as follows [51]:

$$\frac{\partial p_A(a,t)}{\partial t} = -\frac{\partial}{\partial a}\left[\left\{-\frac{\varepsilon\beta_e(a)a}{2} + \frac{\varepsilon\pi S_0}{2a\omega_e^2(a)} + \frac{\varepsilon\pi S_0}{4}\frac{\partial}{\partial a}\left(\frac{1}{\omega_e^2(a)}\right)\right\}p_A(a,t)\right] + \frac{\varepsilon\pi S_0}{2}\frac{\partial^2}{\partial a^2}\left(\frac{p_A(a,t)}{\omega_e^2(a)}\right) \tag{22}$$

where $p_A(a,t)$ is the PDF of the amplitude $A(t)$. Since the initial conditions of the system are $X(0)=0$ and $\dot{X}(0)=0$, the initial amplitude PDF $p_A(a,0)$ is given as

$$p_A(a,0) = \hat{\delta}(a) \tag{23}$$

where $\hat{\delta}(a)$ is the one-sided Dirac delta function, which satisfies

$$\int_0^{\infty} \hat{\delta}(a)da = 1 \tag{24}$$

Finally, the magnitude of the parameter ε of the oscillator in performing the above analysis is mentioned. In Refs. [61] and [62], the stationary response PDFs and transient response statistics of various integer-order nonlinear systems were analyzed by combining the equivalent linearization and the stochastic averaging. It was shown that these PDFs and statistics can be obtained correctly when ε is less than 0.1. Thus, the range of ε for which the combination of the equivalent linearization and the stochastic averaging works well is expected to be $\varepsilon < 0.1$.

5 Complex Fractional Moment Approach

5.1 Conversion of Fokker–Planck Equation to Complex Fractional Moment Equations. From Eq. (18), the equivalent natural frequency $\omega_e(A)$ is represented in the form

$$\omega_e^2(A) = \omega_0^2\{1 + \varepsilon s(A)\} \tag{25}$$

where

$$s(A) = \frac{1}{\pi A}\int_0^{2\pi} g(A\cos\psi)\cos\psi d\psi + \lambda\omega_0^{\alpha-2}\cos\left(\frac{\alpha\pi}{2}\right) \tag{26}$$

Since $\varepsilon \ll 1$, $1/\omega_e^2(A)$ is approximated according to the Maclaurin expansion as follows [51]:

$$\frac{1}{\omega_e^2(A)} = \frac{1}{\omega_0^2\{1 + \varepsilon s(A)\}} \approx \frac{1}{\omega_0^2}\{1 - \varepsilon s(A)\} \tag{27}$$

Substituting Eq. (27) into Eq. (22) leads to

$$\frac{\partial p_A(a,t)}{\partial t} = -\frac{\partial}{\partial a}\left[\left\{-\frac{\varepsilon\beta_e(a)a}{2} + \frac{\varepsilon\pi S_0\{1 - \varepsilon s(a)\}}{2a\omega_0^2} - \frac{\varepsilon^2\pi S_0}{4\omega_0^2}\frac{\partial s(a)}{\partial a}\right\}p_A(a,t)\right] + \frac{\varepsilon\pi S_0}{2\omega_0^2}\frac{\partial^2}{\partial a^2}[\{1 - \varepsilon s(a)\}p_A(a,t)] \tag{28}$$

Because the system nonlinear damping $h(X, \dot{X})$ and nonlinear stiffness $g(X)$ are given in polynomial form, $s(A)$ and $\beta_e(A)$, calculated by Eqs. (19) and (26), respectively, are represented as polynomials in A

$$s(A) = \sum_{j=0}^{n_s} s_j A^j \tag{29}$$

$$\beta_e(A) = \sum_{j=0}^{n_\beta} \beta_j A^j \tag{30}$$

where n_s and n_β are the highest degrees of the polynomials, and s_j and β_j are coefficients. As described in Sec. 4.2, $s(A)$ and

$\beta_e(A)$ have polynomial forms thanks to the approximation of Eqs. (16) and (17) to Eqs. (18) and (19).

The Mellin transform of both sides of Eq. (28) while considering Eqs. (29) and (30) yields

$$\begin{aligned}\frac{\partial}{\partial t}M_{p_A}(\gamma-1,t)=&\frac{\varepsilon}{2}\left\{\sum_{j=0}^{n_\beta}\beta_j\left[a^{\gamma+j}p_A(a,t)\right]_0^\infty-(\gamma-1)\sum_{j=0}^{n_\beta}\beta_j\int_0^\infty a^{\gamma-1+j}p_A(a,t)da\right\}\\&+\frac{\varepsilon\pi S_0}{2\omega_0^2}\left\{\left[a^{\gamma-1}\frac{\partial}{\partial a}p_A(a,t)\right]_0^\infty-\gamma\left[a^{\gamma-2}p_A(a,t)\right]_0^\infty+(\gamma-1)^2\int_0^\infty a^{\gamma-3}p_A(a,t)da\right\}\\&+\frac{\varepsilon^2\pi S_0}{4\omega_0^2}\left\{\sum_{j=0}^{n_s}(2\gamma-j)s_j\left[a^{\gamma-2+j}p_A(a,t)\right]_0^\infty-2\sum_{j=0}^{n_s}s_j\left[a^{\gamma-1+j}\frac{\partial}{\partial a}p_A(a,t)\right]_0^\infty\right.\\&\left.-(\gamma-1)\sum_{j=0}^{n_s}(2\gamma-2+j)s_j\int_0^\infty a^{\gamma-3+j}p_A(a,t)da\right\}\end{aligned}\tag{31}$$

where $M_{p_A}(\gamma-1,t)$ is the amplitude CFM. Herein, it is assumed that for any time t, the amplitude PDF $p_A(a,t)$ does not diverge as $a\to 0$, and $p_A(a,t)$ and $\partial p_A(a,t)/\partial a$ converge to zero faster than power functions of a as $a\to\infty$. These assumptions have been used successfully in CFM-based analyses for various integer-order nonlinear systems [50–53]. Compared to the integer-order systems, the oscillator in Eq. (7) has an additional fractional derivative term, but this term is multiplied by the sufficiently small parameter ε. Thus, it is unlikely that the response of this fractional oscillator is far from the response of the integer-order oscillators. Furthermore, it was recently shown that the stationary amplitude PDF for a fractional linear oscillator under Gaussian white noise (i.e., the special case of Eq. (7) in which $h(X,\dot{X})=0$ and $g(X)=0$) is a Rayleigh distribution [33]. Therefore, the above assumptions about $p_A(a,t)$ seem to be valid even for the fractional nonlinear oscillator given by Eq. (7). Under the assumptions, choosing the real part ρ of γ from the range $2<\rho<\infty$ determined from Eq. (3), the non-integral terms in Eq. (31) disappear, and then, Eq. (31) becomes the governing equation of the time evolution of $M_{p_A}(\gamma-1,t)$

$$\begin{aligned}\frac{\partial}{\partial t}M_{p_A}(\gamma-1,t)=&-\frac{\varepsilon}{2}(\gamma-1)\sum_{j=0}^{n_\beta}\beta_jM_{p_A}(\gamma-1+j,t)\\&+\frac{\varepsilon\pi S_0}{2\omega_0^2}(\gamma-1)^2M_{p_A}(\gamma-3,t)\\&-\frac{\varepsilon^2\pi S_0}{4\omega_0^2}(\gamma-1)\sum_{j=0}^{n_s}(2\gamma-2+j)s_j\\&\times M_{p_A}(\gamma-3+j,t)\end{aligned}\tag{32}$$

5.2 Solving Complex Fractional Moment Equations. Unfortunately, Eq. (32) is not closed due to the existence of multiple CFMs with different real parts of order. As a closure technique, an approximate relation between CFMs with different real parts of order is utilized [46]. Let $\gamma_k^{(l)}=\rho_l+ik\pi/b$ ($l=1,2$; $k=-m,\ -m+1,\ldots,m-1,m$; b and m are defined in Eq. (6)) and the real-part values $\rho_1=\rho$ and $\rho_2=\rho+\Delta\rho$. Then, the following approximate relation between CFMs with different real parts of order is established [46]:

$$\begin{aligned}M_{p_A}(\gamma_s^{(1)}-1,t)&=\sum_{k=-m}^{m}M_{p_A}(\gamma_k^{(2)}-1,t)c_{ks}(\Delta\rho)\\c_{ks}(\Delta\rho)&=\frac{\sin\left[\pi(k-s)-ib\Delta\rho\right]}{\pi(k-s)-ib\Delta\rho}\end{aligned}\tag{33}$$

where $s=-m,\ldots,m$. Thus, $M_{p_A}(\gamma_s^{(1)}-1,t)$ can be approximately represented by $M_{p_A}(\gamma_k^{(2)}-1,t)$. By utilizing Eq. (33), a closed set of CFM linear equations is obtainable. First, $M_{p_A}(\gamma_s-1+j,t)$, $M_{p_A}(\gamma_s-3,t)$ and $M_{p_A}(\gamma_s-3+j,t)$ are rewritten as the linear combination of $M_{p_A}(\gamma_k-1,t)$ ($k=-m,\ldots,m$) using Eq. (33). Next, substituting them into Eq. (32) discretized as $\gamma=\gamma_s$ ($=\rho+is\pi/b,\ s=-m,\ldots,m$) leads to $(2m+1)$ linear ordinary differential equations for $M_{p_A}(\gamma_s-1,t)$ ($s=-m,\ldots,m$).

$$\begin{aligned}\frac{\partial}{\partial t}M_{p_A}(\gamma_s-1,t)=&-\frac{\varepsilon}{2}(\gamma_s-1)\sum_{j=0}^{n_\beta}\beta_j\sum_{k=-m}^{m}M_{p_A}(\gamma_k-1,t)c_{ks}(-j)\\&+\frac{\varepsilon\pi S_0}{2\omega_0^2}(\gamma_s-1)^2\sum_{k=-m}^{m}M_{p_A}(\gamma_k-1,t)c_{ks}(2)\\&-\frac{\varepsilon^2\pi S_0}{4\omega_0^2}(\gamma_s-1)\sum_{j=0}^{n_s}(2\gamma_s-2+j)s_j\\&\times\sum_{k=-m}^{m}M_{p_A}(\gamma_k-1,t)c_{ks}(2-j)\end{aligned}\tag{34}$$

In solving Eq. (34), it is necessary to impose a constraint that corresponds to the normalization condition for a PDF, which is given by [46]

$$\begin{aligned}&M_{p_A}(\gamma_0-1,t)\\&=\frac{1-\rho}{e^{b(1-\rho)}-e^{-b(1-\rho)}}\left[2b-\sum_{\substack{k=-m\\k\neq 0}}^{m}\frac{e^{b(1-\gamma_k)}-e^{-b(1-\gamma_k)}}{1-\gamma_k}M_{p_A}(\gamma_k-1,t)\right]\end{aligned}\tag{35}$$

Combining Eqs. (34) and (35), we anew obtain 2 m coupled linear differential equations for $M_{p_A}(\gamma_s-1,t)$ ($s=-m,\ldots,-1,1,\ldots,m$), which are solved with the initial condition given by

$$M_{p_A}(\gamma_s-1,0)=\int_0^\infty p_A(a,0)a^{\gamma_s-1}da=0\tag{36}$$

where $p_A(a,0)=\hat{\delta}(a)$.

In this way, the solution of the FP equation (22) is attained in terms of CFMs by solving Eqs. (34)–(36). The computation time is only a few seconds. When performing a stationary response analysis, linear algebraic equations derived by setting the time derivative term in Eq. (34) to zero are solved in conjunction with Eq. (35).

5.3 Calculation of Response Probability Density Function. The amplitude PDF $p_A(a,t)$ is acquired by substituting the CFMs $M_{p_A}(\gamma_s-1,t)$ ($s=-m,\ldots,m$) determined from Eqs. (34)–(36) into Eq. (6). The joint PDF $p_{X\dot{X}}(x,\dot{x},t)$ of displacement $X(t)$ and

velocity $\dot{X}(t)$ is also obtained as

$$p_{X\dot{X}}(x, \dot{x}, t) = \frac{1}{2\pi} p_A(a, t)|J| \tag{37}$$

where J is the Jacobian of variable transformation pertaining to the pseudo-harmonic representation (10), and $|J|$ is given by [51]

$$|J| = \frac{1}{\omega_e(a)a - \frac{d}{da}\left(\frac{1}{\omega_e(a)}\right)\dot{x}^2} \tag{38}$$

Equations (37) and (38) include a. For this a, substitute the solution for a of the following equation:

$$a = \sqrt{x^2 + \frac{\dot{x}^2}{\omega_e^2(a)}} \tag{39}$$

By way of example, let us consider the case of $g(X) = X^3$. From Eq. (18), $\omega_e^2(A)$ is derived as

$$\omega_e^2(A) = \omega_0^2\left(1 + \frac{3}{4}\varepsilon A^2\right) + \varepsilon\lambda\omega_0^\alpha \cos\left(\frac{\alpha\pi}{2}\right) \tag{40}$$

Then, $|J|$ and a are

$$|J| = \frac{4\omega_e^3(a)}{\left\{4\omega_e^4(a) + 3\varepsilon\omega_0^2\dot{x}^2\right\}a}$$
$$a = \sqrt{\frac{2}{3\varepsilon}\left\{\sqrt{\left(C + \frac{3}{4}\varepsilon x^2\right)^2 + 3\varepsilon\frac{\dot{x}^2}{\omega_0^2}} + \frac{3}{4}\varepsilon x^2 - C\right\}} \tag{41}$$

where

$$C = 1 + \varepsilon\lambda\omega_0^{\alpha-2}\cos\left(\frac{\alpha\pi}{2}\right)$$

The displacement PDF $p_X(x, t)$ and the velocity PDF $p_{\dot{X}}(\dot{x}, t)$ are determined as the marginal PDFs of $p_{X\dot{X}}(x, \dot{x}, t)$.

5.4 Summary of Analytical Procedure. In Secs. 4 and 5, the derivation process for the equations used in the present analysis was described in detail. However, when applying the present approach, it is not necessary to perform all of the analyses in Secs. 4 and 5 in sequence. The actual analysis consists of fewer equations and procedures. The practical analytical procedure is summarized as follows:

(1) Calculate the equivalent natural frequency $\omega_e(A)$ and the equivalent damping coefficient $\beta_e(A)$ using Eqs. (18) and (19). $\omega_e^2(A)$ is given in the form of Eqs. (25) and (29), while $\beta_e(A)$ is given in the form of Eq. (30).
(2) Substitute $\omega_e(A)$ and $\beta_e(A)$ into Eq. (34) to get the linear ordinary differential equations for amplitude CFMs $M_{p_A}(\gamma_s - 1, t)$ $(s = -m, \ldots, -1, 1, \ldots, m)$.
(3) Solve Eq. (34) in combination with Eq. (35) and the initial condition given by Eq. (36) to determine $M_{p_A}(\gamma_s - 1, t)$ $(s = -m, \ldots, m)$.
(4) Apply the inverse Mellin transform to $M_{p_A}(\gamma_s - 1, t)$, i.e., substitute $M_{p_A}(\gamma_s - 1, t)$ into Eq. (6) to obtain the amplitude PDF $p_A(a, t)$.
(5) Calculate a and $|J|$ in the joint PDF $p_{X\dot{X}}(x, \dot{x}, t)$ of $X(t)$ and $\dot{X}(t)$ in Eq. (37) via Eqs. (38) and (39).
(6) Substitute $p_A(a, t)$, a, and $|J|$ into Eq. (37) to obtain $p_{X\dot{X}}(x, \dot{x}, t)$.

6 Numerical Examples

The accuracy and versatility of the present analytical approach are assessed through numerical examples of three linear and nonlinear oscillators with fractional derivative elements. To the best of the author's knowledge, no exact PDF solution has yet been found for oscillators with fractional derivatives, even for stationary responses. For this reason, the analytical results of response PDFs are compared with the results of the pertinent MCS.

6.1 Linear Oscillator With Fractional Derivative Element. First, to verify the effectiveness of the present approach for dynamic systems involving fractional-order derivatives, a linear oscillator with a fractional derivative element is considered, once ignoring nonlinearities. The equation of motion is given by

$$\ddot{X} + \varepsilon\lambda D_{0,t}^\alpha X + \omega_0^2 X = \varepsilon^{\frac{1}{2}} W(t) \tag{42}$$

that corresponds to the case of $h(X, \dot{X}) = 0$ and $g(X) = 0$ in Eq. (7).

Using Eqs. (18) and (19), $\omega_e(A)$ and $\beta_e(A)$ are calculated as

$$\omega_e^2(A) = \omega_e^2 = \omega_0^2 + \varepsilon\lambda\omega_0^\alpha \cos\left(\frac{\alpha\pi}{2}\right)$$
$$\beta_e(A) = \beta_e = \lambda\omega_0^{\alpha-1}\sin\left(\frac{\alpha\pi}{2}\right) \tag{43}$$

Since there is no nonlinear element in the system, these equivalent coefficients do not depend on the amplitude $A(t)$. The linear differential equations for amplitude CFMs to be solved are derived from Eqs. (34) and (43) as

$$\frac{\partial}{\partial t}M_{p_A}(\gamma_s - 1, t) = -\frac{\varepsilon\lambda\omega_0^{\alpha-1}}{2}\sin\left(\frac{\alpha\pi}{2}\right)(\gamma_s - 1)M_{p_A}(\gamma_s - 1, t)$$
$$+ \frac{\varepsilon\pi S_0}{2\omega_0^2}\left\{1 - \varepsilon\lambda\omega_0^{\alpha-2}\cos\left(\frac{\alpha\pi}{2}\right)\right\}$$
$$\times(\gamma_s - 1)^2 \sum_{k=-m}^{m} M_{p_A}(\gamma_k - 1, t)c_{ks}(2) \tag{44}$$

where $s = -m, \ldots, -1, 1, \ldots m$. Equation (44) is solved in combination with Eq. (35) and the initial condition given by Eq. (36). Then, the discretized inverse Mellin transform (Eq. (6)) of the resulting CFMs $M_{p_A}(\gamma_s - 1, t)$ $(s = -m, \ldots, m)$ yields the amplitude PDF $p_A(a, t)$. Further, the joint PDF $p_{X\dot{X}}(x, \dot{x}, t)$ of $X(t)$ and $\dot{X}(t)$ is obtained by Eq. (37). From Eqs. (38) and (39), a and $|J|$ in Eq. (37) are

$$a = \sqrt{x^2 + \frac{\dot{x}^2}{\omega_e^2}}; \quad |J| = \frac{1}{\omega_e a} \tag{45}$$

where ω_e is given by Eq. (43).

The reliability of the analytical method is validated with three different values of the fractional derivative order α: $\alpha = 0.3$, 0.5, and 0.7. It is known that $0.3 \le \alpha \le 0.7$ is frequently adopted as the best fitting value in modeling the dynamic properties of viscoelastic materials [11–15]. For this reason, the above three values are used for the fractional order. Other system and excitation parameters are set as $\omega_0 = 1$, $\varepsilon = 0.01$, $\lambda = 7$, and $S_0 = 1$. Further, $\Delta\eta = 0.3$, $\rho = 3.7$, and $m = 220$ are adopted in solving Eq. (44).

For comparisons of the analytical results with simulation results, MCS is performed on Eq. (42). The difficulty inherent in simulations of fractional-order systems is that the fractional derivatives depend on the entire past time history of the system response, as can be seen from Eq. (8). As an efficient and accurate numerical technique, this study utilizes a method to approximately convert an equation of motion including fractional-order derivatives into a set of integer-order differential equations [63]. A brief summary of this methodology is provided in Appendix. Once the integer-order differential equations are obtained, standard numerical integration algorithms can be used to generate realizations of the system response. In this study, the fourth-order Runge–Kutta method is employed. The time increment size Δt for the numerical integration is $\Delta t = 10^{-4}$. MCS results are computed from 5×10^6 realizations. Δt and the number of realizations were chosen based on a preliminary study in order to obtain as accurate a solution as

possible, since the MCS results are used as substitutes for the true response PDFs of the oscillator. The computer system used in the MCS has an Intel Core i9-10,900 K CPU with 32 GB RAM, and the operating system is Microsoft Windows 10. The source code for the MCS was prepared using the c language, which was compiled with the GNU compiler collection (version 12.3). The simulation method described herein is also adopted in the second and third examples shown later.

In Fig. 1, the PDFs $p_A(a, t)$, $p_X(x, t)$, and $p_{\dot{X}}(\dot{x}, t)$ of amplitude $A(t)$, displacement $X(t)$, and velocity $\dot{X}(t)$ for the case of $\alpha = 0.5$ are shown. The solid lines indicate the analytical results, whereas the discrete symbols denote the pertinent MCS results. The three times in the figure were chosen to show the early phase of the response, the stationary phase and a phase in between the two, while also taking into account the ease of viewing the figure. From the standpoint of evaluating system reliability, it is crucial to obtain the tails of response PDFs with high accuracy. Therefore, semi-log plots of $p_X(x, t)$ and $p_{\dot{X}}(\dot{x}, t)$ are also presented to confirm the agreement between the analytical and MCS results in the tail region. The results of $p_A(a, t)$ demonstrate the validity of the assumptions about $p_A(a, t)$ used in deriving Eq. (32) from Eq. (31). Slight deviations can be seen in the peaks of the displacement and velocity PDFs. However, the accuracy of the analytical results is overall quite satisfactory, including the tail region. Although not shown in the figure, good agreement was also achieved for the cases of $\alpha = 0.3$ and $\alpha = 0.7$ (some results are provided in Fig. 2). Additionally, the authors also carefully checked the validity for various other values of α in the range $0 < \alpha < 1$, and the analytical method accurately yielded transient response PDF solutions for any α, including the cases of $\alpha = 0.1$ and 0.9.

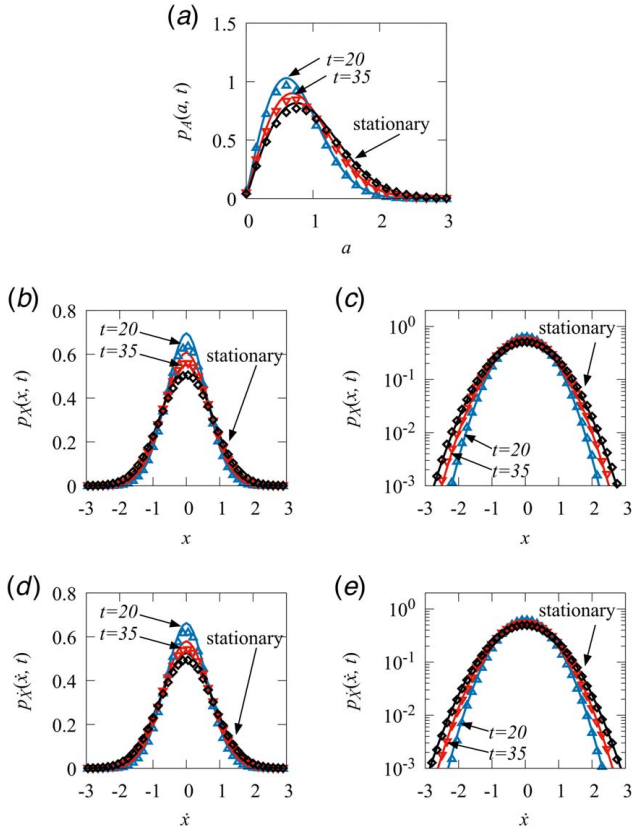

Fig. 1 Transient and stationary response PDFs of a linear oscillator with a fractional derivative of order 0.5. Solid lines: present analysis. Discrete symbols: MCS. (*a*) amplitude, (*b*) displacement, (*c*) displacement (semi-log plot), (*d*) velocity, and (*e*) velocity (semi-log plot).

Figure 2 shows a comparison of displacement and velocity PDFs between the three types of fractional order α. The following tendencies can be observed in the response PDFs for larger α:

(i) The widths of the PDFs are narrower (i.e., their variance decreases).
(ii) They reach stationary PDFs faster.

The reason for the above is that as α approaches 1, the contribution of the fractional derivative element to viscous damping increases. The present method accurately predicts such changes in the response PDF depending on the fractional order α.

Finally, the computation time for the present analytical method was 2.7 s, whereas the MCS took about 25 h (the computation times were similar in the second and third examples shown later as well). Thus, the computational time was significantly reduced compared to the corresponding MCS.

6.2 Oscillator With Fractional Derivative Element and Nonlinearities in Both Damping and Stiffness. The applicability to systems that have not only fractional derivatives but also nonlinearities is illustrated. Let $h(X, \dot{X}) = \delta_1\dot{X} + \delta_3\dot{X}^3$ and $g(X) = \kappa_3X^3 + \kappa_5X^5$, and a fractional nonlinear oscillator with cubic nonlinearity in damping and cubic and quintic nonlinearities in stiffness is considered, whose motion is governed by

$$\ddot{X} + \varepsilon\lambda D^{\alpha}_{0,t}X + \varepsilon(\delta_1\dot{X} + \delta_3\dot{X}^3) + \omega_0^2X + \varepsilon\omega_0^2(\kappa_3X^3 + \kappa_5X^5) = \varepsilon^{\frac{1}{2}}W(t) \tag{46}$$

$\omega_e(A)$ and $\beta_e(A)$ for this system are

$$\omega_e^2(A) = \omega_0^2\left\{1 + \varepsilon\left(\frac{3}{4}\kappa_3A^2 + \frac{5}{8}\kappa_5A^4\right)\right\} + \varepsilon\lambda\omega_0^{\alpha}\cos\left(\frac{\alpha\pi}{2}\right)$$

$$\beta_e(A) = \delta_1 + \frac{3}{4}\delta_3\omega_0^2\left[A^2 + \varepsilon\left\{\lambda\omega_0^{\alpha-2}\cos\left(\frac{\alpha\pi}{2}\right)A^2 + \frac{3}{4}\kappa_3A^4 + \frac{5}{8}\kappa_5A^6\right\}\right] + \lambda\omega_0^{\alpha-1}\sin\left(\frac{\alpha\pi}{2}\right) \tag{47}$$

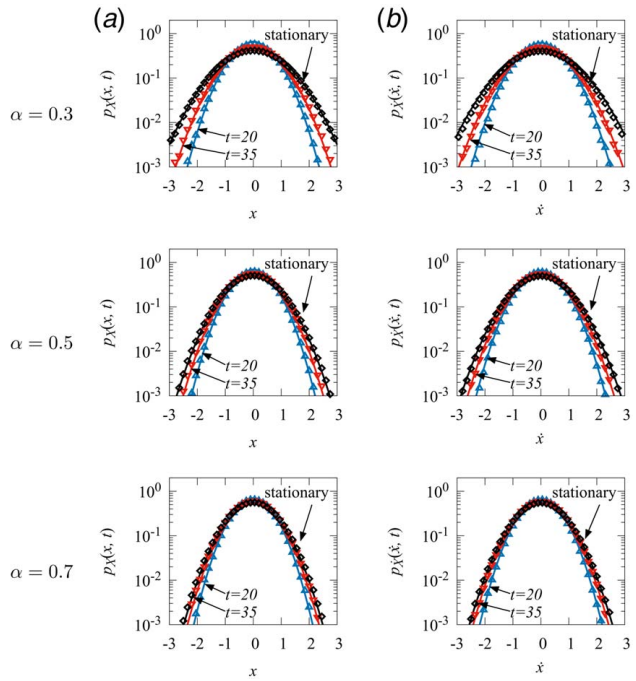

Fig. 2 Comparison of response PDFs between three types of fractional order α. Solid lines: present analysis. Discrete symbols: MCS. (*a*) displacement and (*b*) velocity.

The governing equations for amplitude CFMs are written in the form

$$\frac{\partial}{\partial t}M_{p_A}(\gamma_s-1,t)=-\frac{\varepsilon}{2}\left\{\delta_1+\lambda\omega_0^{\alpha-1}\sin\left(\frac{\alpha\pi}{2}\right)\right\}(\gamma_s-1)M_{p_A}(\gamma_s-1,t)$$
$$-\frac{3\varepsilon\delta_3\omega_0^2}{8}\left\{1+\varepsilon\lambda\omega_0^{\alpha-2}\cos\left(\frac{\alpha\pi}{2}\right)\right\}(\gamma_s-1)$$
$$\times\sum_{k=-m}^{m}M_{p_A}(\gamma_k-1,t)c_{ks}(-2)$$
$$-\frac{9\varepsilon^2\delta_3\kappa_3\omega_0^2}{32}(\gamma_s-1)\sum_{k=-m}^{m}M_{p_A}(\gamma_k-1,t)c_{ks}(-4)$$
$$-\frac{15\varepsilon^2\delta_3\kappa_5\omega_0^2}{64}(\gamma_s-1)\sum_{k=-m}^{m}M_{p_A}(\gamma_k-1,t)c_{ks}(-6)$$
$$+\frac{\varepsilon\pi S_0}{2\omega_0^2}\left\{1-\varepsilon\lambda\omega_0^{\alpha-2}\cos\left(\frac{\alpha\pi}{2}\right)\right\}(\gamma_s-1)^2$$
$$\times\sum_{k=-m}^{m}M_{p_A}(\gamma_k-1,t)c_{ks}(2)$$
$$-\frac{3\varepsilon^2\pi\kappa_3 S_0}{8\omega_0^2}\gamma_s(\gamma_s-1)M_{p_A}(\gamma_s-1,t)$$
$$-\frac{5\varepsilon^2\pi\kappa_5 S_0}{16\omega_0^2}(\gamma_s^2-1)\sum_{k=-m}^{m}M_{p_A}(\gamma_k-1,t)c_{ks}(-2) \quad (48)$$

where $s=-m,\ldots,-1,1,\ldots m$. Equation (48) is solved with Eqs. (35) and (36). Equations (38) and (47) lead to $|J|$ in the joint PDF $p_{X\dot{X}}(x,\dot{x},t)$ of Eq. (37) as

$$|J|=\frac{4\omega_e^3(a)}{\left\{4\omega_e^4(a)+3\varepsilon\kappa_3\omega_0^2\dot{x}^2+5\varepsilon\kappa_5\omega_0^2\dot{x}^2a^2\right\}a} \quad (49)$$

For a in Eqs. (37) and (49), the square root of the solution of the following cubic equation for a^2 is used

$$\frac{5}{8}\varepsilon\kappa_5 a^6+\frac{\varepsilon}{4}\left(3\kappa_3-\frac{5}{2}\kappa_5x^2\right)a^4+\left(C-\frac{3}{4}\varepsilon\kappa_3x^2\right)a^2-\left(Cx^2+\frac{\dot{x}^2}{\omega_0^2}\right)=0 \quad (50)$$

where

$$C=1+\varepsilon\lambda\omega_0^{\alpha-2}\cos\left(\frac{\alpha\pi}{2}\right)$$

Equation (50) is derived from Eqs. (39) and (47).

The following parameter values are used: $\omega_0=1$, $\varepsilon=0.01$, $\lambda=7$, $\alpha=0.5$, $\delta_1=8$, $\delta_3=8$, $\kappa_3=1$, $\kappa_5=1$, and $S_0=1$. The parameters when solving Eq. (48) are given by $\Delta\eta=0.5$, $\rho=3.7$, and $m=220$.

Figure 3 displays the analytical results of transient and stationary response PDFs and the corresponding MCS results. There are small errors in the peaks of the displacement and velocity PDFs for the initial short time period, but otherwise the analytical results are in good agreement with the simulation results, including the tail region. The results of the amplitude PDF $p_A(a, t)$ show that the assumptions about $p_A(a, t)$ are valid for the system containing nonlinearities as well. Further, a comparison of Figs. 1 and 3 reveals

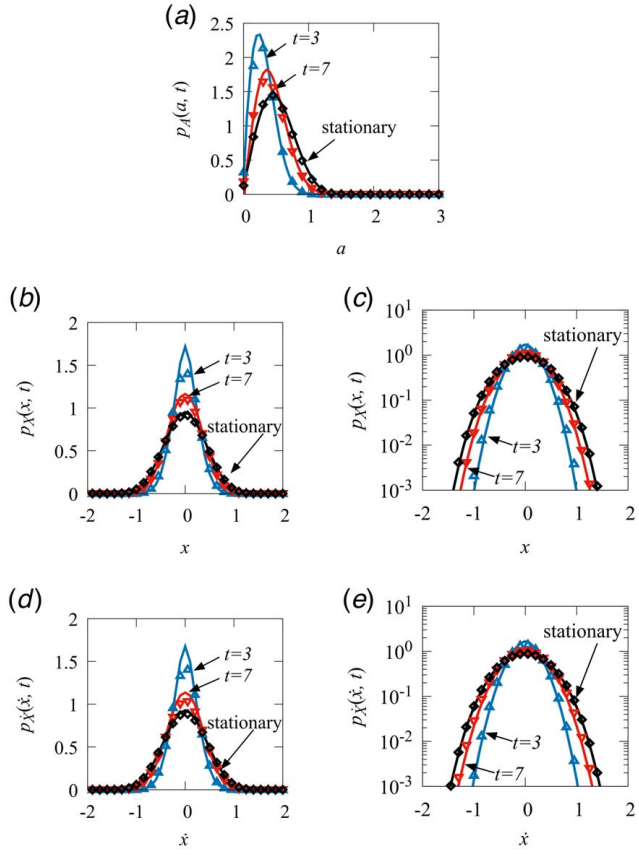

Fig. 3 Transient and stationary response PDFs of a oscillator with a fractional derivative element and nonlinearities in both damping and stiffness. Solid lines: present analysis. Discrete symbols: MCS. (*a*) amplitude, (*b*) displacement, (c) displacement (semi-log plot), (*d*) velocity, and (e) velocity (semi-log plot).

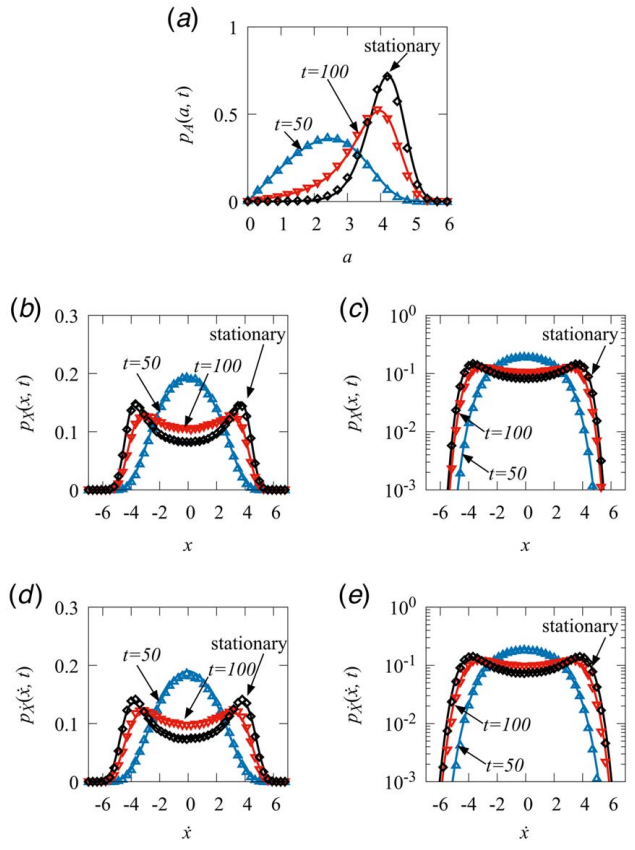

Fig. 4 Transient and stationary response PDFs of a Duffing-van der Pol oscillator with a fractional derivative element. Solid lines: present analysis. Discrete symbols: MCS. (*a*) amplitude, (*b*) displacement, (c) displacement (semi-log plot), (*d*) velocity, and (*e*) velocity (semi-log plot).

that the response PDFs in this example are narrower than those of the linear oscillator with same α. This is because the nonlinear damping and nonlinear stiffness of the system behave to suppress large responses. The analytical result accurately captures such a narrowed PDF shape caused by the system nonlinearities. Thus, the present analytical method is able to provide accurate solutions even for a system with nonlinear damping and nonlinear stiffness as well as a fractional derivative element.

6.3 Duffing-van der Pol Oscillator With Fractional Derivative Element. Finally, an example of a fractional nonlinear oscillator that exhibits limit-cycle behavior is presented in order to further demonstrate the versatility of the present method. Consider a Duffing-van der Pol oscillator with a fractional derivative element, whose equation of motion is described by

$$\ddot{X} + \varepsilon\lambda D^{\alpha}_{0,t}X + \varepsilon(\delta_1 + \delta_3 X^2)\dot{X} + \omega_0^2 X + \varepsilon\omega_0^2 X^3 = \varepsilon^{\frac{1}{2}} W(t) \tag{51}$$

which corresponds to the case of $h(X, \dot{X}) = \delta_1\dot{X} + \delta_3 X^2\dot{X}$, and $g(X) = X^3$ in Eq. (7).

For this system, $\omega_e(A)$ and $\beta_e(A)$ are given by

$$\begin{aligned}\omega_e^2(A) &= \omega_0^2\left(1 + \frac{3}{4}\varepsilon A^2\right) + \varepsilon\lambda\omega_0^{\alpha}\cos\left(\frac{\alpha\pi}{2}\right)\\ \beta_e(A) &= \delta_1 + \frac{1}{4}\delta_3 A^2 + \lambda\omega_0^{\alpha-1}\sin\left(\frac{\alpha\pi}{2}\right)\end{aligned} \tag{52}$$

The differential equations for amplitude CFMs are

$$\begin{aligned}\frac{\partial}{\partial t}M_{p_A}(\gamma_s - 1, t) = &-\frac{\varepsilon}{2}\left\{\delta_1 + \lambda\omega_0^{\alpha-1}\sin\left(\frac{\alpha\pi}{2}\right)\right\}(\gamma_s - 1)M_{p_A}(\gamma_s - 1, t)\\ &-\frac{\varepsilon\delta_3}{8}(\gamma_s - 1)\sum_{k=-m}^{m} M_{p_A}(\gamma_k - 1, t)c_{ks}(-2)\\ &+\frac{\varepsilon\pi S_0}{2\omega_0^2}\left\{1 - \varepsilon\lambda\omega_0^{\alpha-2}\cos\left(\frac{\alpha\pi}{2}\right)\right\}(\gamma_s - 1)^2\\ &\times\sum_{k=-m}^{m} M_{p_A}(\gamma_k - 1, t)c_{ks}(2)\\ &-\frac{3\varepsilon^2\pi S_0}{8\omega_0^2}\gamma_s(\gamma_s - 1)M_{p_A}(\gamma_s - 1, t)\end{aligned} \tag{53}$$

where $s = -m, \ldots, -1, 1, \ldots m$. Equation (53) is solved with Eqs. (35) and (36). Since the nonlinear stiffness term of this system is $g(X) = X^3$, a and $|J|$ in the joint PDF $p_{X\dot{X}}(x, \dot{x}, t)$ of Eq. (37) are given by Eq. (41).

The linear damping coefficient δ_1 is set as $\delta_1 = -5$ so that the oscillator (51) takes diffusive limit-cycle motion. The other parameter values are chosen as $\omega_0 = 1$, $\varepsilon = 0.01$, $\lambda = 1$, $\alpha = 0.5$, $\delta_3 = 1$, and $S_0 = 1$. Further, $\Delta\eta = 0.5$, $\rho = 3.7$, and $m = 220$ are used when solving Eq. (53).

The analytical results of response PDFs and the corresponding MCS results for comparison are depicted in Fig. 4. The oscillator behavior approaches diffusive limit-cycle motion with time. Accordingly, the displacement and velocity PDFs change from unimodal shapes to bimodal ones. It can be seen that the present analytical technique estimates such highly non-Gaussian PDFs and the time evolution of their shapes with high accuracy. Furthermore, due to the behavior of diffusive limit cycle, the amplitude PDF also has a unique shape that is different from the PDFs in the previous two examples. Nevertheless, the assumptions about the amplitude PDF are still valid in this example.

7 Conclusions

A CFM-based analysis has been performed for obtaining the transient response PDF of nonlinear oscillators with fractional derivative elements under Gaussian white noise. The oscillators have polynomial-type nonlinearities in both stiffness and damping.

First, the equivalent natural frequency and equivalent damping coefficient of the oscillator were determined. The fractional derivative element of the oscillator contributes to both elasticity and viscosity. For this reason, the equivalent coefficients need to be determined by taking account of not only the effects of nonlinearities but also the contributions of the fractional element. Furthermore, the coefficients must be given in polynomial form of response amplitude to utilize the CFM-based approach. This paper proposed formulas to determine the equivalent coefficients that satisfy the above requirements, based on an equivalent linearization technique. Then, the FP equation was derived using stochastic averaging. Further, by the use of the Mellin transform and the relation between CFMs with different real parts of order, the FP equation was converted into a set of linear ordinary differential equations for amplitude CFMs. Solving it combined with a constraint that corresponds to the normalization condition for a PDF, the amplitude CFMs were obtained. Finally, the inverse Mellin transform of the resulting CFMs yielded the amplitude PDF. The joint PDF of displacement and velocity was also attained from the amplitude PDF.

In numerical examples, three linear and nonlinear oscillators with fractional derivatives have been considered to demonstrate the accuracy and versatility of the present analytical technique. It has been shown that the present method accurately determines the shapes of response PDFs that vary depending on both the fractional order and nonlinearities of the oscillator.

The practical importance of acquiring response PDFs is that system reliability can be assessed from the PDF. Therefore, it is highly significant to perform reliability analysis of fractional nonlinear systems using response PDF solutions obtained by the present analytical technique. Such a study would also be an effective and practical way to quantitatively evaluate the accuracy of the present analytical method. This topic will be addressed in our future work.

Acknowledgment

This work was supported by JSPS KAKENHI Grant No. JP21K03944.

Conflict of Interest

The authors have no competing interests to declare that are relevant to the content of this paper.

Data Availability Statement

The datasets generated and supporting the findings of this article are obtainable from the corresponding author upon reasonable request.

Appendix

This appendix provides a brief summary of a method to approximately convert an equation of motion including fractional derivative elements into a set of integer-order differential equations, which is used in MCS. Readers interested in more details of the methodology are referred to Ref. [63].

The gamma function $\Gamma(\alpha)$ is defined as

$$\Gamma(\alpha) = \int_0^{\infty} e^{-z} z^{\alpha-1} dz \tag{A1}$$

It is known that $\Gamma(\alpha)$ satisfies the following identity:

$$\Gamma(\alpha)\Gamma(1-\alpha)=\frac{\pi}{\sin(\pi\alpha)} \tag{A2}$$

By employing Eqs. (A1) and (A2), the α-order Caputo fractional derivative (8) can be rewritten in the form

$$D^{\alpha}_{0,t}X(t)=\frac{\sin(\alpha\pi)}{\pi}\int_0^t\int_0^{\infty}e^{-z}z^{\alpha-1}(t-s)^{-\alpha}\dot{X}(s)dzds \tag{A3}$$

Performing a variable transformation $z=(t-s)y^2$, we obtain

$$D^{\alpha}_{0,t}X(t)=\frac{2\sin(\alpha\pi)}{\pi}\int_0^{\infty}y^{2\alpha-1}\left\{\int_0^t e^{-(t-s)y^2}\dot{X}(s)ds\right\}dy \tag{A4}$$

Herein, the following variable is introduced:

$$\Phi(y,\,t)=y^{2\alpha-1}\int_0^t e^{-(t-s)y^2}\dot{X}(s)ds \tag{A5}$$

Then, Eq. (A4) is written as

$$D^{\alpha}_{0,t}X(t)=\mu\int_0^{\infty}\Phi(y,\,t)dy \tag{A6}$$

where $\mu=2\sin(\pi\alpha)/\pi$. Further, from Eq. (A5), $\Phi(y,\,t)$ is the solution of the following first-order ordinary differential equation:

$$\frac{d}{dt}\Phi(y,\,t)=-y^2\Phi(y,\,t)+y^{2\alpha-1}\dot{X}(t) \tag{A7}$$

with zero initial condition $\Phi(y,\,0)=0$.

In order to obtain an efficient and accurate numerical scheme, the integral in Eq. (A6) is discretized by utilizing the Gauss–Jacobi quadrature. To this aim, the following variable transformation is used for Eq. (A6):

$$u=\frac{1-y}{1+y} \tag{A8}$$

Then, Eq. (A6) becomes

$$D^{\alpha}_{0,t}X(t)=\mu\int_{-1}^{1}(1-u)^{2\alpha-1}(1+u)^{1-2\alpha}\bar{\Phi}(u,\,t)du \tag{A9}$$

where

$$\bar{\Phi}(u,\,t)=2(1-u)^{1-2\alpha}(1+u)^{2\alpha-3}\Phi\left(\frac{1-u}{1+u},\,t\right) \tag{A10}$$

Next, the Gauss–Jacobi quadrature is applied to Eq. (A9).

$$D^{\alpha}_{0,t}X(t)=\mu\int_{-1}^{1}(1-u)^{2\alpha-1}(1+u)^{1-2\alpha}\bar{\Phi}(u,\,t)du\simeq\mu\sum_{i=1}^{n}w_i\bar{\Phi}(u_i,\,t) \tag{A11}$$

where u_i is the nodal point determined as the ith root of the Jacobi polynomial $P_n^{(2\alpha-1,1-2\alpha)}(u)$, whose definition is

$$P_n^{(2\alpha-1,1-2\alpha)}(u)=\frac{(-1)^n}{2^n n!(1-u)^{2\alpha-1}(1+u)^{1-2\alpha}}\times\frac{d^n}{du^n}\left[(1-u)^{2\alpha-1+n}(1+u)^{1-2\alpha+n}\right] \tag{A12}$$

w_i is the weight computed as

$$w_i=-\frac{2\Gamma(n+2\alpha)\Gamma(n+2-2\alpha)}{\Gamma(n+1)(n+1)!P_n^{(2\alpha-1,1-2\alpha)\prime}(u_i)P_{n+1}^{(2\alpha-1,1-2\alpha)}(u_i)} \tag{A13}$$

where $P_n^{(2\alpha-1,1-2\alpha)\prime}(u_i)$ denotes the first-order derivative of $P_n^{(2\alpha-1,1-2\alpha)}(u_i)$. From Eqs. (A10) and (A7), we have

$$\bar{\Phi}(u_i,\,t)=2(1-u_i)^{1-2\alpha}(1+u_i)^{2\alpha-3}\Phi\left(\frac{1-u_i}{1+u_i},\,t\right) \tag{A14}$$

$$\frac{d}{dt}\Phi(y_i,\,t)=-y_i^2\Phi(y_i,\,t)+y_i^{2\alpha-1}\dot{X}(t),\qquad y_i=\frac{1-u_i}{1+u_i} \tag{A15}$$

To summarize the above, Eq. (7) can be approximated as follows:

$$\ddot{X}+\varepsilon\lambda\mu\sum_{i=1}^{n}2w_i(1-u_i)^{1-2\alpha}(1+u_i)^{2\alpha-3}\Phi(y_i,\,t)+\varepsilon h(X,\,\dot{X})+\omega_0^2X(t)+\varepsilon\omega_0^2g(X)=\varepsilon^{\frac{1}{2}}W(t) \tag{A16}$$

where the time evolution of $\Phi(y_i,\,t)$ is governed by Eq. (A15). Further, Eq. (A16) is recast in the form

$$\frac{dX}{dt}=\dot{X} \tag{A17}$$

$$\frac{d\dot{X}}{dt}=-\varepsilon\lambda\mu\sum_{i=1}^{n}2w_i(1-u_i)^{1-2\alpha}(1+u_i)^{2\alpha-3}\Phi(y_i,\,t)-\varepsilon h(X,\,\dot{X})-\omega_0^2X(t)-\varepsilon\omega_0^2g(X)+\varepsilon^{\frac{1}{2}}W(t) \tag{A18}$$

In this manner, the system equation of motion with a fractional derivative term is approximately converted into a set of $(n+2)$ first-order ordinary differential equations consisting of Eqs. (A15), (A17), and (A18). In this study, n was selected as $n=10$, and thus, 12 simultaneous equations were solved using the fourth-order Runge–Kutta scheme.

References

[1] Lin, Y. K., and Cai, G. Q., 1995, *Probabilistic Structural Dynamics*, McGraw-Hill, New York.

[2] Podlubny, I., 1999, *Fractional Differential Equations: An Introduction to Fractional Derivatives, Fractional Differential Equations, to Methods of Their Solution and Some of Their Applications*, Academic Press, San Diego, CA.

[3] Hilfer, R., 2000, *Applications Of Fractional Calculus in Physics*, World Scientific, Singapore.

[4] Sabatier, J., Agrawal, O. P., and Tenreiro Machado, J. A., 2000, *Advances in Fractional Calculus: Theoretical Developments and Applications in Physics and Engineering*, Springer, Dordrecht.

[5] Mainardi, F., 2010, *Fractional Calculus and Waves in Linear Viscoelasticity: An Introduction to Mathematical Models*, Imperial College Press, London.

[6] Atanackovic, T. M., Pilipovic, S., Stankovic, B., and Zorica, D., 2010, *Fractional Calculus With Applications in Mechanics: Vibrations and Diffusion Processes*, Wiley, London.

[7] Herrmann, R., 2018, *Fractional Calculus: An Introduction for Physicists*, 3rd ed., World Scientific, Singapore.

[8] Rossikhin, Y. A., and Shitikova, M. V., 1997, "Applications of Fractional Calculus to Dynamic Problems of Linear and Nonlinear Hereditary Mechanics of Solids," ASME Appl. Mech. Rev., **50**(1), pp. 15–67.

[9] Rossikhin, Y. A. and Shitikova, M. V., 2010, "Application of Fractional Calculus for Dynamic Problems of Solid Mechanics: Novel Trends and Recent Results," ASME Appl. Mech. Rev., **63**(1), p. 010801.

[10] Sun, H. G., Zhang, Y., Baleanu, D., Chen, W., and Chen, Y. Q., 2018, "A New Collection of Real World Applications of Fractional Calculus in Science and Engineering," Commun. Nonlinear Sci. Numer. Simul., **64**(1), pp. 213–231.

[11] Jones, D. I. G., 2001, *Handbook of Viscoelastic Vibration Damping*, Wiley, New York.

[12] Bagley, R. L., and Torvik, P. J., 1983, "Fractional Calculus – A Different Approach to the Analysis of Viscoelastically Damped Structures," AIAA J., **21**(5), pp. 741–748.

[13] Torvik, P. J., and Bagley, R. L., 1984, "On the Appearance of the Fractional Derivative in the Behavior of Real Materials," ASME J. Appl. Mech., **51**(2), pp. 294–298.

[14] Bagley, R. L., and Torvik, P. J., 1985, "Fractional Calculus in the Transient Analysis of Viscoelastically Damped Structures," AIAA J., **23**(6), pp. 918–925.

[15] Bagley, R. L., and Torvik, P. J., 1986, "On the Fractional Calculus Model of Viscoelastic Behavior," J. Rheol., **30**(1), pp. 133–155.

[16] Koh, C. G., and Kelly, J. M., 1990, "Application of Fractional Derivatives to Seismic Analysis of Base-Isolated Models," Earthq. Eng. Struct. Dyn., **19**(2), pp. 229–241.

[17] Sasso, M., Palmieri, G., and Amodio, D., 2011, "Application of Fractional Derivative Models in Linear Viscoelastic Problems," Mech. Time-Depend. Mater., **15**(1), pp. 367–387.

[18] Di Paola, M., Pirrotta, A., and Valenza, A., 2011, "Visco-Elastic Behavior Through Fractional Calculus: An Easier Method for Best Fitting Experimental Results," Mech. Mater., **43**(12), pp. 799–806.
[19] Makris, N., and Constantinou, M. C., 1992, "Spring-Viscous Damper Systems for Combined Seismic and Vibration Isolation," Earthq. Eng. Struct. Dyn., **21**(8), pp. 649–664.
[20] Lee, H. H., and Tsai, C.-S., 1994, "Analytical Model of Viscoelastic Dampers for Seismic Mitigation of Structures," Comput. Struct., **50**(1), pp. 111–121.
[21] Shen, K. L., and Soong, T. T., 1995, "Modeling of Viscoelastic Dampers for Structural Applications," J. Eng. Mech., **121**(6), pp. 694–701.
[22] Rüdinger, F., 2006, "Tuned Mass Damper With Fractional Derivative Damping," Eng. Struct., **28**(13), pp. 1774–1779.
[23] Singh, M. P., Chang, T.-S., and Nandan, H., 2011, "Algorithms for Seismic Analysis of MDOF Systems With Fractional Derivatives," Eng. Struct., **33**(8), pp. 2371–2381.
[24] Agrawal, O. P., 2001, "Stochastic Analysis of Dynamic Systems Containing Fractional Derivatives," J. Sound Vib., **247**(5), pp. 927–938.
[25] Huang, Z. L., Jin, X. L., Lim, C. W., and Wang, Y., 2010, "Statistical Analysis for Stochastic Systems Including Fractional Derivatives," Nonlinear Dyn., **59**(1), pp. 339–349.
[26] Cao, Q., Hu, S.-L. J., and Li, H., 2021, "Nonstationary Response Statistics of Fractional Oscillators to Evolutionary Stochastic Excitation," Commun. Nonlinear Sci. Numer. Simul., **103**(1), p. 105962.
[27] Di Paola, M., Failla, G., and Pirrotta, A., 2012, "Stationary and Non-Stationary Stochastic Response of Linear Fractional Viscoelastic Systems," Probab. Eng. Mech., **28**(1), pp. 85–90.
[28] Spanos, P. D., and Zhang, W., 2022, "Nonstationary Stochastic Response Determination of Nonlinear Oscillators Endowed With Fractional Derivatives," Int. J. Non-Linear Mech., **146**(1), p. 104170.
[29] Zhang, W., Spanos, P. D., and Di Matteo, A., 2023, "Nonstationary Stochastic Response of Hysteretic Systems Endowed With Fractional Derivative Elements," ASME J. Appl. Mech., **90**(6), p. 061011.
[30] Spanos, P. D., and Evangelatos, G. I., 2010, "Response of a Non-Linear System With Restoring Forces Governed by Fractional Derivatives - Time Domain Simulation and Statistical Linearization Solution," Soil Dyn. Earthq. Eng., **30**(9), pp. 811–821.
[31] Kong, F., Zhang, H., Zhang, Y., Chao, P., and He, W., 2022, "Stationary Response Determination of MDOF Fractional Nonlinear Systems Subjected to Combined Colored Noise and Periodic Excitation," Commun. Nonlinear Sci. Numer. Simul., **110**(1), p. 106392.
[32] Kong, F., Han, R., and Zhang, Y., 2022, "Approximate Stochastic Response of Hysteretic System With Fractional Element and Subjected to Combined Stochastic and Periodic Excitation," Nonlinear Dyn., **107**(1), pp. 375–390.
[33] Spanos, P. D., Kougioumtzoglou, I. A., dos Santos, K. R. M, and Beck, A. T., 2018, "Stochastic Averaging of Nonlinear Oscillators: Hilbert Transform Perspective," J. Eng. Mech., **144**(2), p. 04017173.
[34] Huang, Z. L., and Jin, X. L., 2009, "Response and Stability of a SDOF Strongly Nonlinear Stochastic System With Light Damping Modeled by a Fractional Derivative," J. Sound Vib., **319**(3), pp. 1121–1135.
[35] Hu, F., Chen, L. C., and Zhu, W. Q., 2012, "Stationary Response of Strongly Non-Linear Oscillator With Fractional Derivative Damping Under Bounded Noise Excitation," Int. J. Non-Linear Mech., **47**(10), pp. 1081–1087.
[36] Yang, Y., Xu, W., Gu, X., and Sun, Y., 2015, "Stochastic Response of a Class of Self-Excited Systems With Caputo-Type Fractional Derivative Driven by Gaussian White Noise," Chaos Solit. Fractals, **77**(1), pp. 190–204.
[37] Wang, D., Xu, W., Gu, X., and Pei, H., 2016, "Response Analysis of Nonlinear Vibro-Impact System Coupled With Viscoelastic Force Under Colored Noise Excitations," Int. J. Non-Linear Mech., **86**(1), pp. 55–65.
[38] Xiao, Y., Xu, W., and Wang, L., 2016, "Stochastic Responses of Van Der Pol Vibro-Impact System With Fractional Derivative Damping Excited by Gaussian White Noise," Chaos, **26**(1), p. 033110.
[39] Ning, X., Ma, Y., Li, S., Zhang, J., and Li, Y., 2018, "Response of Non-Linear Oscillator Driven by Fractional Derivative Term Under Gaussian White Noise," Chaos Solit. Fractals, **113**(1), pp. 102–107.
[40] Yang, Y.-G., and Xu, W., 2018, "Stochastic Analysis of Monostable Vibration Energy Harvesters With Fractional Derivative Damping Under Gaussian White Noise Excitation," Nonlinear Dyn., **94**(1), pp. 639–648.
[41] Sun, Y.-H., Yang, Y.-G., Zhang, Y., and Xu, W., 2021, "Probabilistic Response of a Fractional-Order Hybrid Vibration Energy Harvester Driven by Random Excitation," Chaos, **31**(1), p. 013111.
[42] Di Matteo, A., 2023, "Response of Nonlinear Oscillators With Fractional Derivative Elements Under Evolutionary Stochastic Excitations: A Path Integral Approach Based on Laplace's Method of Integration," Probab. Eng. Mech., **71**(1), p. 103402.
[43] Fragkoulis, V. C., Kougioumtzoglou, I. A., Pantelous, A. A., and Beer, M., 2019, "Non-Stationary Response Statistics of Nonlinear Oscillators With Fractional Derivative Elements Under Evolutionary Stochastic Excitation," Nonlinear Dyn., **97**(1), pp. 2291–2303.
[44] Cottone, G., Di Paola, M., and Metzler, R., 2010, "Fractional Calculus Approach to the Statistical Characterization of Random Variables and Vectors," Physica A, **389**(5), pp. 909–920.
[45] Di Paola, M., and Pinnola, F. P., 2012, "Riesz Fractional Integrals and Complex Fractional Moments for the Probabilistic Characterization of Random Variables," Probab. Eng. Mech., **29**(1), pp. 149–156.
[46] Di Paola, M., 2014, "Fokker Planck Equation Solved in Terms of Complex Fractional Moments," Probab. Eng. Mech., **38**(1), pp. 70–76.
[47] Di Matteo, A., Di Paola, M., and Pirrotta, A., 2014, "Probabilistic Characterization of Nonlinear Systems Under Poisson White Noise Via Complex Fractional Moments," Nonlinear Dyn., **77**(1), pp. 729–738.
[48] Alotta, G., and Di Paola, M., 2015, "Probabilistic Characterization of Nonlinear Systems Under α-stable White Noise Via Complex Fractional Moments," Physica A, **420**(1), pp. 265–276.
[49] Itoh, D., Tsuchida, T., and Kimura, K., 2018, "An Analysis of a Nonlinear System Excited by Combined Gaussian and Poisson White Noises Using Complex Fractional Moments," Theor. and Appl. Mech. Japan, **64**(1), pp. 103–114.
[50] Jin, X., Wang, Y., Huang, Z., and Di Paola, M., 2014, "Constructing Transient Response Probability Density of Non-Linear System Through Complex Fractional Moments," Int. J. Nonlinear Mech., **65**(1), pp. 253–259.
[51] Itoh, D., and Tsuchida, T., 2022, "Transient Response Analysis of a System With Nonlinear Stiffness and Nonlinear Damping Excited by Gaussian White Noise Based on Complex Fractional Moments," Acta Mech., **233**(1), pp. 2781–2796.
[52] Xie, X., Li, J., Liu, D., and Guo, R., 2017, "Transient Response of Nonlinear Vibro-Impact System Under Gaussian White Noise Excitation Through Complex Fractional Moments," Acta Mech., **228**(1), pp. 1153–1163.
[53] Niu, L., Xu, W., and Guo, Q., 2021, "Transient Response of the Time-Delay System Excited by Gaussian Noise Based on Complex Fractional Moments," Chaos, **31**(1), p. 053111.
[54] Dalzell, J. E., 1978, "A Note on the Form of Ship Roll Damping," J. Ship Res., **22**(1), pp. 178–185.
[55] Muscolino, G., Ricciardi, G., and Vasta, M., 1997, "Stationary and Non-Stationary Probability Density Function for Non-Linear Oscillators," Int. J. Nonlinear Mech., **32**(6), pp. 1051–1064.
[56] Roberts, J. B., and Spanos, P. D., 2003, *Random Vibration and Statistical Linearization*, Dover Publications, New York.
[57] Spanos, P. D., Di Matteo, A., Cheng, Y., Pirrotta, A., and Li, J., 2016, "Galerkin Scheme-Based Determination of Survival Probability of Oscillators With Fractional Derivative Elements," ASME J. Appl. Mech., **83**(12), p. 121003.
[58] Di Matteo, A., Spanos, P. D., and Pirrotta, A., 2018, "Approximate Survival Probability Determination of Hysteretic Systems With Fractional Derivative Elements," Probab. Eng. Mech., **54**(1), pp. 138–146.
[59] Roberts, J. B., and Spanos, P. D., 1986, "Stochastic Averaging: An Approximate Method of Solving Random Vibration Problems," Int. J. Nonlinear Mech., **21**(2), pp. 111–134.
[60] Stratonovich, R. L., 1986, *Topics in the Theory of Random Noise, Vols. 1 and 2*, Gordon & Breach, New York.
[61] Spanos, P.-T. D., 1976, "Linearization Techniques for Non-Linear Dynamical Systems," Earthquake Engineering Research Laboratory, California Institute of Technology, Report No. EERL 7Q-04.
[62] Iwan, W. D., and Spanos, P.-T. D., 1978, "Response Envelope Statistics for Nonlinear Oscillators With Random Excitation," ASME J. Appl. Mech., **45**(1), pp. 170–174.
[63] Diethelm, K., 2008, "An Investigation of Some Nonclassical Methods for the Numerical Approximation of Caputo-Type Fractional Derivatives," Numer. Algor., **47**(1), pp. 361–390.